Insights into the local and non-local interaction of two species on the impact of the Allee Predator-prey Model using Holling type II Functional Response

Tahani Al-Karkhi[a]

[a]*Mathematical Sciences Department, University of Essex, Wivenhoe Park, CO4 9FS, Essex, UK.*

Abstract

There is currently much interest in predator–prey models across a variety of bioscientific disciplines. The focus is on quantifying predator–prey interactions, and this quantification is being formulated especially as regards climate change. In this article, a stability analysis is used to analyse the behaviour of a general two-species model with respect to the Allee effect (on the growth rate and nutrient limitation level of the prey population). We present a description of the local and non-local interaction stability of the model and detail the types of bifurcation which arise, proving that there is a Hopf bifurcation in the Allee effect module. A stable periodic oscillation was encountered which was due to the Allee effect on the prey species. As a result of this, the positive equilibrium of the model could change from stable to unstable and then back to stable, as the strength of the Allee effect (or the 'handling' time taken by predators when predating) increased continuously from zero. Hopf bifurcation has arose yield some complex patterns that have not been observed previously in predator-prey models, and these, at the same time, reflect long term behaviours. These findings have significant implications for ecological studies, not least with respect to examining the mobility of the two species involved in the non-local domain using Turing instability. A spiral generated by local interaction (reflecting the instability that forms even when an infinitely large carrying capacity is assumed) is used in the model.

DOI : 10.5121/mathsj.2023.10204

Keywords: Prey and predator, Bifurcation analysis, Hopf bifurcation, Patterns formation, Turing instability, Turing Hopf bifurcation, Reaction -diffusion.

1. Introduction

The value of positive interactions, such as can be represented as Allee effects, which are intended to allow members of a predator species to capture large prey via cooperative hunting and group living may be significant in locations which have an abundance of large prey. However, it was seen by Alonso *et al.* [2002] that Turing mechanisms may generate patchiness in an otherwise homogeneous environment under certain conditions of trophic interaction and predator–prey relative diffusion. Baurmann [2004] showed that various different patterns can appear at different depths, and by using a model involving nutrients and microorganisms in sediments, they proved that the formation of spatio–temporal patterns can be the consequence of interactions between predation and transport processes. Therefore, here, we study reaction diffusion systems to determine the Turing spaces for a given model. Thereafter, a bifurcation analysis of a specific pattern formation is established Elragig [2012]. It should also be noted that reactivity is vital for Turing instability to arise; the presence of short term periodicity behaviour indicates that disturbances to a stable equilibrium will eventually diminish. At first the size of such disturbances grows rapidly, and this growth continues for a while, but eventually it decays Neubert [2002]. The local and global extinction levels increase with an increasing Allee effect. However, there are only a few articles in the literature which have observed the influence of the Allee effect in relation to stabilizing or destabilizing the predator–prey system Zu [2010], Zhou [2005], Kent [2003], Ferdy [2002]. The Allee effect refers to a depensation or inverse density dependence Liermann [2001] which occurs when a per capita fertility rate decrease leads to low population densities. The consequences of the Allee effect may occur under special circumstances such as the following: when there are difficulties in finding mates because the population density is low Zu [2010]; social dysfunction as a result of small

population sizes; and increased predation risk due to failing flocking or schooling behaviours Zu [2010], Groom [1998], Courchamp [1999], kuussaari [1998] and Zhou [2005] combined a mathematical analysis with a numerical simulation in order to prove the presence of the Allee effect within a predator-prey system. The classifications of the functional responses present in predator–prey models can be summarised as follows; prey-dependent and predator-dependent. A prey-dependent functional response means that the response is a function only of the prey's density, while a predator-dependent functional response means that the response is a function of both the prey and the predator densities. In this article we examine the Holling type II functional response when the prey dependent component is predominant; the predator–prey model using a Holling type II functional response is the most realistic. However, the impact of the Allee effect on the stability of a system governed by a Holling type II functional response has been, up to now, poorly understood both empirically and theoretically Zu [2010]. Numerous studies looking at pattern formation in the behaviours of reaction diffusion models of prey predator interaction have been carried out: In Turing [1990], Edwards [1996], Alonso *et al.* [2002], Haque, Mainul [2011] and Sambath [2016]. The present article will explore Turing instability; this is a concept developed by Alan Turing, who suggested that morphogens, a term given to a system of reacting and diffusing chemicals, can generate patterns from a previously uniform state Elragig [2012]. Gambino [2013] demonstrates that a steady state can be considered to be Turing unstable, if it is unstable as a solution to the full reaction diffusion system but stable as a solution to the reaction system without diffusion. This aforementioned situation results in the formation of spatial patterns. The presence of dispersal affects the behaviours of spatial perturbations which do not decay to zero, and this results in Turing instability Neubert [2002]. Here we investigate the Turing instability of non-linear reaction diffusion systems which exhibit various different diffusion types. Although Turing instability has been covered quite comprehensively by previous researchers Rodrigues [2011], here, we wish to show that the coexistence point is stable for a reaction only system but is unstable for a reaction diffusion

system, depending on the prevalence of any Allee effects in operations θ value. Moreover, in our study, a perturbation with a given wave number is applied to obtain a dispersion relation.

This article is arranged as follows. The first section introduces our study by looking at a temporal version of the predator-prey model. The second section considers a qualitative analysis of a reaction model in order to present an analysis of the equilibrium points present and show the nullclines of the system. In the next section we derive the Turing conditions and then the amplitude equation. In the later sections, we present both the uniform and the non-uniform solutions with regard to the aforementioned, using a numerical exploration of reaction diffusion models; this helps us to introduce the main finding of the present research.

2. General model and description

In this section, we describe a general local interaction of the two species model under the influence of a pre-specified Allee parameter value θ, where this θ represents the Allee effect on the prey population.

$$\begin{aligned} \frac{\partial x}{\partial t} &= F(x,y) + D_x \frac{\partial^2 x}{\partial X^2} \\ \frac{\partial y}{\partial t} &= G(x,y) + D_y \frac{\partial^2 y}{\partial X^2} \end{aligned} \tag{1}$$

where $F(x,y)$ and $G(x,y)$ are defined as follows:

$$F(x,y) = x\left(\frac{r}{\theta + x} - \delta x - \frac{x}{k}\right) - \frac{mxy}{ax + c} \tag{2}$$

$$G(x,y) = \frac{emxy}{ax + c} - dy \tag{3}$$

To start introducing our predator–prey model, supporting the Allee effect, some important justifications need to be stated such as x and y describes the prey and predator densities in the closed homogeneous system represented by the model system of 1. $D_x = D_y = 0$ in this section. Let the first term of $F(x,y)$ be the growth (fertility) rate of a species that has x adults in an isolated patch,

then the fertility rate increases with population density as described by Eq.2. where Allee effects θ is taken into account in order to form the assumption that the prey population grows semi-logistically. The values governing this growth are r (the intrinsic growth rate), and k (the carrying capacity). Self-shading and nutrient limitations directly determine this latter value (the carrying capacity). Furthermore, θ and δ are the Allee effect parameters used to describe the behaviour of prey productivity and the impact of the Allee effect on the prey species' mortality. The parameter r refers to the per capita maximum growth rate of the species Ferdy [2002], Zu [2010]. The bigger θ is, the stronger the Allee effect is considered to be. If the nutrient limitation (carrying capacity) is low then the prey population will extend i.e, we either obtain a relatively small or a negative equilibrium. On the other hand, if the value of k is high, then this will positively impact the type of equilibrium present. The second term of the function $F(x, y)$ and first term of $G(x, y)$ are both Holling type II functional response and the second term of $G(x, y)$ is the linear mortality function of predators.

The model in Eq.(2) and Eq.(3), has x and y as the densities of prey and predator populations respectively, in the closed homogeneous system that we are modelling. The prey population in Eq.(2)is assumed to grow semi logistically under the influence of the Allee effect θ with an intrinsic rate of growth of r and a carrying capacity of k, where the carrying capacity corresponds to the influences of nutrient limitation and self-shading. θ and δ are the Allee effect parameter used to describe the behaviour of prey productivity and the impact of the Allee effect on prey species mortality. The Allee affect as represented by the above parameters resulted in the population of the prey, x, exceeding the value of the carrying capacity, k, and biologically this is not possible. The predator population grazes on the prey population according to a Holling type II functional response, which is a hyperbolic function and represents the fact predation saturates at high prey densities because of the time it takes to handle prey. Whereby the rate of grazing saturates at high densities of prey. Prey biomass is converted to predator biomass with an efficiency of m. When food

densities are low, and when these are at half-saturation a, this situation is represented by the parameter, e. When there are no (or very low levels of) defense mechanism present, it can be said that the mortality of the predator species is mostly caused by predation (on the predators) by higher trophic predators. However, other eventualities such as sinking is also factors, and these factors are included in the value of d. Hence the term can represent the increased mortality due to predation. The parameter values used are experimental parameter. The

Table 1: Variable and parameter definitions and the values used for the model given by Eqs.(3) and (2)

Parameter	Value	Unit
r	$0-5$	day^{-1}
k	$0-1000$	$\mu g\ CI^{-1}$
a	1.9	$\mu g\ CI^{-1}\ \text{day}^{-1}$
c	2.5	$\mu g\ CI^{-1}$
e	1.5	day^{-1}
m	0.75	day^{-1}
θ	$0-3.5$	day^{-1}
δ	$0-0.7$	day^{-1}
d	0.03	day^{-1}

parameter m, θ and δ they includes both the natural predator mortality and the effects of high predation feeding on the predator species in the absence of prey defense mechanism; such as the chemical release when the predation is high on prey.

3. Qualitative Analysis of The Equilibria

The system in Eq.(2) and Eq.(3) possesses three different equilibria, table 2 exhibits the stability of each of these equilibria.

- The eigenvalues analysis of the predator prey dynamics therefore leads

Table 2: Biologically relevant possible equilibria of the system given by the Eqs.(3) and (2)

Equilibrium	Definition	Value in parametrized system	Description	Types of Equilibrium
E_0	(x_e, y_e)	$(0, 0)$	Trivial (extinct)	unstable saddle node $(\frac{r}{\theta}, -d)$
E_1	(x_e, y_e)	$((k\delta - 1)x^2 + (k\delta - 1)\theta x - rk, 0)$	prey equilibrium	unstable saddle node as in Eq.(4) and (5)
E_3	(x_e, y_e)	Eq.(6)	Coexistence point	stable focus (Hopf bifurcation)

to the following conclusions: the model's trivial steady state is a unstable saddle node as $\lambda_1 = \frac{r}{\theta}$ and $\lambda_2 = -d$ are the eigenvalues. The two eigenvalues are distinct; the extinct point is stable.

- The prey equilibrium, $((k\delta - 1)x^2 + (k\delta - 1)\theta x - rk, 0)$, is a quadratic equation with two real roots and each root has two real eigenvalues with distinct signs; the equilibrium is stable focus and the eigenvalues are given in Eqs.(4) and (5).

$$\lambda_1 = \frac{a_0 + \sqrt{k^2\delta^2\theta^2 + 4k^2r\delta - 2k\delta\theta^2 - 4kr + \theta^2}(ad - em) - em\theta - 2cd + d\theta}{ka\delta\theta + 2kc\delta + \sqrt{k^2\delta^2\theta^2 + 4k^2r\delta - 2k\delta\theta^2 - 4kr + \theta^2} - a\theta + a - 2c} \tag{4}$$

$$\lambda_2 = \frac{a_1 - \sqrt{a_2}(8k^2\delta^2\theta^4 + 5k^2r\delta\theta^2 + 16k\delta\theta^4 - 2k^2r^2 - 5kr\theta^2}{2\sqrt{k^2\delta^2\theta^2 + 4k^2r\delta - 2k\delta\theta^2 - 4kr + \theta^2})} \tag{5}$$

Where a_0,a_1 and a_2 are cascading parameters given in the appendix.

- The coexistence equilibrium is given by Eq.(6). It has an interesting behaviour when $0 < \theta < 3.5$ and $0 < \delta < 0.75$. The system exhibits stable focus when the two Allee affect parameters are in this range and Hopf bifurcation occurred with pure imaginary eigenvalues when $\delta = 0.3565$ and $\theta = 2.5$.

$$x = \frac{cd}{(em - ad)},$$
$$y = \frac{c^2de(kadr\delta - kemr - ad\theta\delta + em\theta\delta + cd)}{k(a^3d^3\theta - 3a^2d^2em\theta + 3ade^2m^2\theta - e^3m^3\theta - a^2cd^3 + 2acd^2em - cde^2m^2)} \tag{6}$$

The prey coexistence equilibrium in Eq.(6) is positive when $(kadr\delta - kemr > ad\theta\delta + em\theta\delta + cd)$, and this is using the parameter values given

in table 1. Also, the predator-prey equilibrium in Eq.(6) is positive when the numerator $(kadr - kemr - ad\theta + em\theta + cd) > 0$ and the denominator is

$$k(a^3d^3\theta - 3a^2d^2em\theta + 3ade^2m^2\theta) > (e^3m^3\theta - a^2cd^3 + 2acd^2em - cde^2m^2)$$

These findings have implications for ecological studies, not least they reflect in detail, the location and the number of the roots and their type: when the system exhibits Hopf bifurcations. The presence of the Allee effect cautions us that, in terms of nature preservation, if either or both of the prey or predators to be protected are subject to a $(\theta > 0)$ and $\delta > 0$. Allee effect and consequently have $k(a^3d^3\theta - 3a^2d^2em\theta + 3ade^2m^2\theta) > 0$, the measures taken must take this into account Zu [2010]. If the numbers of either prey or predators are lower than a certain value range, the respective species will become extinct (within the environment studied). Allee effects with respect to different species, due to their different mechanisms, may affect the dynamics of the respective populations differently Zhou [2005]. The correspondent eigenvalues of Eq.(6) are given by the Eq.(7), which is a quartic polynomial of θ:

$$\lambda_{1,2} = \frac{1}{2}\alpha \pm \sqrt{\beta} \tag{7}$$

The eigenvalues in Eq.(7) are complex with α and β are cascading parameters that have a hierarchical relationship with each other. they are presented in the Appendix of this article. The system will exhibit two different behaviours with respect to increases in the value of θ.

Fig.(1) depicts the system nullclines, in Fig(a) there are two intersections in this figure; these correspond to $\theta = 3.5$ and the type of these equilibrium are stable focus as shown in Fig(b) and (c); in addition, increasing θ value will result in the system exhibiting unstable nodes. Any further alteration to the parameter values will lead to negative populations for both species and this is biologically irrelevant, especially if we increase them as follows: $\theta > 3.5$, $\delta > 0.75$ and $c > 2.5$, leaving the other parameters as in table 1.

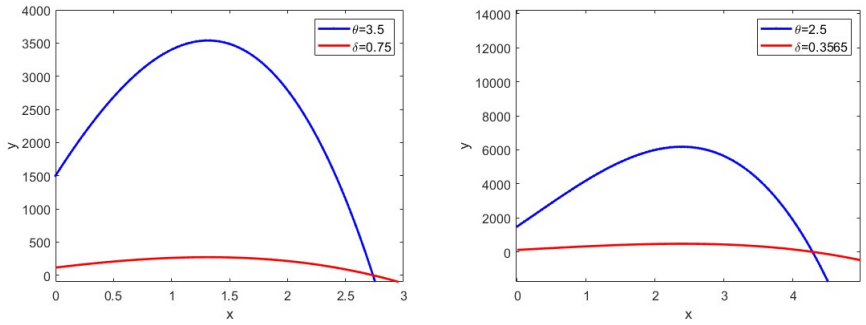

(a) (b)

Figure 1: The nullclines of the system given in Eq.(2 and 3). The blue and red curves represent the non-trivial nullclines for prey and predators, respectively. The blue curve represents the prey nullcline, while the red curve represents the predator nullcline. Fig (a) illustrate the situation when $\theta = 3.5$ and $\delta = 0.75$ show an intersections; that occur at the points where the system exhibits stable focus equilibrium at the coexistence point. Fig(b) represent the Hopf bifurcation point when $\theta = 2.5$ and $\delta = 0.3565$.

The corresponding behaviour of the model represented by Eq.(2 and 3) in terms of time evolution is given by Fig.(2). In the situations represented by all the sub-figures—Fig.(2(a)), Fig.(2(c)), Fig.(2(d)) and Fig.(2(e))— all the parameters are fixed as in table 1 so that all the correspondence equilibria, such as $x = 0.091603$, $y = 6.79184$ when $\theta = 1.5, 2.5, 3.5$, lie in the horizontal line and the spiral of both predator and prey represents an stable focus behaviour which took place in between $100 - 200$ seconds and was related to improvements in both species' conditions of existence under minor Allee effects: value $\theta = 0.5$ and $\theta = 1.5$ for predator and prey, respectively. The system behaviour in Fig. (2(a)) reflects the instability that can take place even when an infinitely large carrying capacity $k = 120$ is used in the model. When the value of θ is increased to 1.5 as in Fig.(2(c)) the system exhibits an stable focus and both predator and prey population persist indefinitely. Therefore, all the trajectories are drawn to the point $x = 0.091603$ and $y = 6.5785853$.

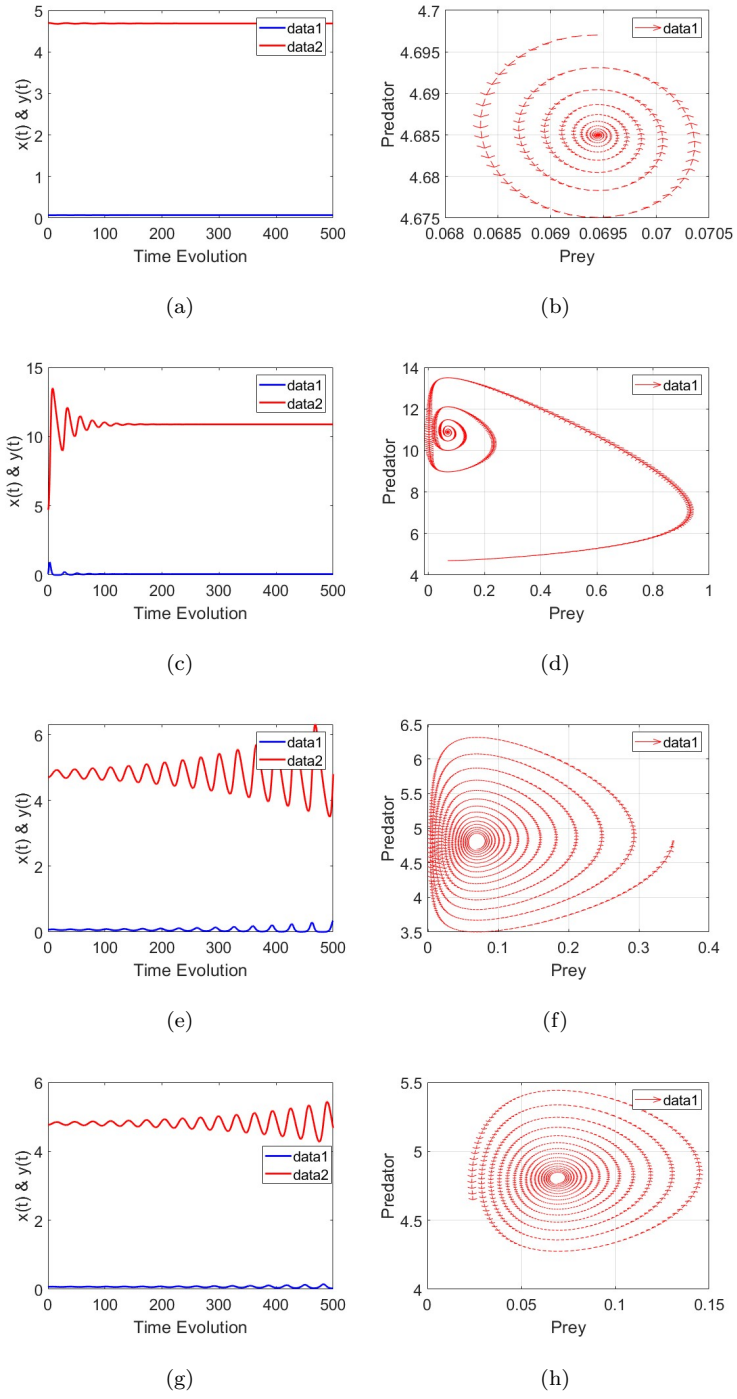

Figure 2: Evolution over time simulation to show the behavior of the non-spatial model represented by Eq.(2 and Eq.(3). In Fig.(2(a)) the system exhibits an stable focus point w.r.t $\theta = 3.5$ and $\delta = 0.75$.Decreasing the value of θ to $\theta = 1.5$ and fix $\delta = 0.75$, the system keeps exhibiting the same behaviour. All trajectories are drawn to the correspondence equilibrium, as in Fig.(2(c)) and fig2(d). Fig 2(d) shows the system behaviour when we fixed the value of $\theta = 3.5$ and decreased $\delta = 0.25$: one of the equilibria vanish and we end up with one stable eigenvalue (which means the system will exhibit Hopf bifurcation as shown in Fig.(2(h) and 2(g)).

4. The behaviour of the non-spatial model

We first consider the mathematical model in Eq.(1) in the absence of diffusion, i.e. $D_x = D_y = 0$; for this situation, the bifurcation diagram for both species x and y is depicted in Fig.(3).

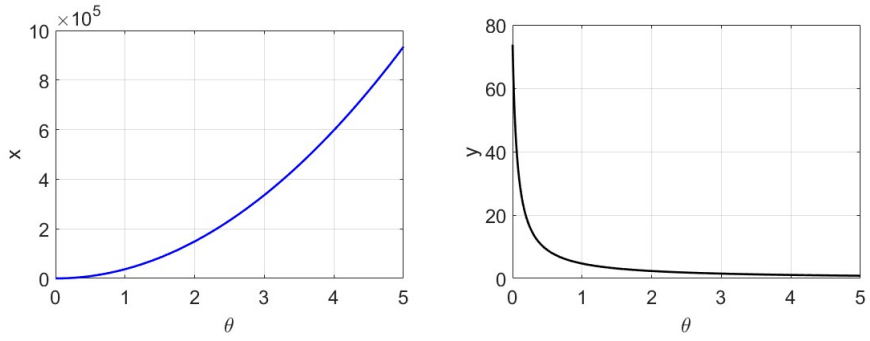

(a) (b)

Figure 3: The bifurcation diagram of the system in Eq.(2) and Eq.(3) depicts $x\&y$ when $0 < \theta < 3.5$. In 3(a) we studied the bifurcation in the E_1, which is the prey equilibrium with respect to θ, while in 3(b) we studied the bifurcation in E_3, which is the coexistence point with respect to $\theta = 3.5$ and $\delta = 0.25$.

In Fig.(3) we explore the effects of changing θ on the system's stability we utilities the parameter values given in subsection 2 to clarify the system behaviour and to show where exactly we found Hopf bifurcation. In Fig 3(a) we studies the stability of E_1 w.r.t θ this equilibrium is a quadratic equation and it's two roots are prey only equilibrium. The first root is relevant and with stable focus eigenvalues, as the second root was biologically irrelevant . As the model represented by Eq.(2) and Eq.(3) provides a suitable framework for further exploration, we also studied the system stability w.r.t θ in E_3, which is the coexistence equilibrium and at this point the system exhibit Hopf bifurcation when $\theta = 3.5$ and $\delta = 0.25$ as in Fig.2(d). It can readily be seen that the carrying capacity is a very important parameter in relation to each model as it specifies the maximum values of the population densities for prey, x and predator, y, and determines the various different stability conditions corresponding to each

θ and δ the Allee affects. An increase in the predator grazing of prey led to an increase in the predator mortality rate, under the Allee effect θ. This is assumed to be as a result of increased predation by high trophic predators (due to the effects of prey defense mechanism).

Theorem 4.1. Assume $\delta > 0.7$. ODE system undergoes Hopf bifurcation at $(\delta_H, (x_1, y_1))$, where $\delta_H = \dfrac{\sqrt{\delta(k\delta - 1)r}}{\delta}$.

Proof. Conditions for Hopf bifurcation to occur in the system are as follows:
(i) A purely imaginary roots were observed in the system, i.e. $T_0 = 0, J_0 > 0$;
(ii) Transversality condition: $\left.\dfrac{dRe(\lambda)}{d\delta}\right|_{\delta=\delta_H} \neq 0$.
From $T_0 = a_{11} + a_{22}$, we obtain $\delta = \delta_H$ $\delta_H = \frac{a_{11}\theta^2 + a_2\theta - a_{13}}{(ad-em)\theta - cd)^2 kcd}$. Where, $a_{11} = -2a^2cd^3 + 4 + acd^2em - 2 + cde^2m^2$, $a_{22} = ke^3d^3r - 3ka^2d^2emr + 3kade^2m^2r - ke^3m^3r + 4ac^2d^3 - 4c^2d^2em$, and $a_{13} = 2c^3d^3$. When $\delta > \delta_H, T_0 < 0$, the corresponding ordinary differential system is asymptotically stable; when $\delta < \delta_H, T_0 > 0$ (here, $\theta > 3.5$ is required), the corresponding non-spatial model is stable. Therefore, when $\delta = \delta_H, T_0 = 0$, the system occurs Hopf bifurcation near (x_1, y_1). Moreover, in advantage of $\mathrm{Re}(\lambda) = \dfrac{T_0}{2}$ the system will keep oscillate in a stable orbit.

5. Numerical Exploration of the Reaction Diffusion Model in 1 and 2 Dimensions

After we developed the spatial model from the non-spatial model by adding the spatial derivative, in Eq.(1), we then studied the Turing mechanisms which are in effect in the augmented model, so as to discover at what points and under what conditions we obtain Turing patterns. We also performed some numerical simulations in order to understand the behaviour of the reaction diffusion model.

5.1. Uniform solutions and linear stability

The multitrophic predator–prey model, Eq.(1), has uniform solutions $x(X, t) = x_e$ and $y(X, t) = y_e$, which are given by Eq.(6). To determine the linear stability of the uniform solutions, we use the dispersion relation in Eq.(19), for which all

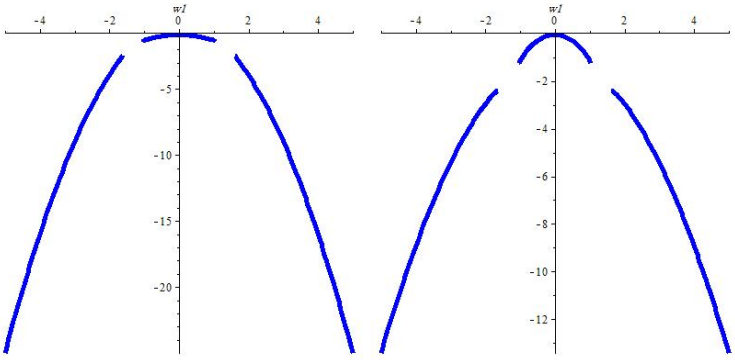

(a) (b)

Figure 4: The type of the eigenvalues (stable focus) in one dimension when $\theta = 3.5$ and $K = 120$, which represents the pair of complex eigenvalues which is yielded when the diffusion parameter values are $D_x < D_y$ and the wave number is between $-5 < w < 5$.

partial derivatives are given in section (4). From Eq.(19), a uniform solution is said to be stable when $\delta(w) \leq 0$ for $\forall w \in \mathbb{R}$ and unstable where $\exists w$ such that $\delta(w) > 0$. So, the maximum of the spectrum, Eq.(8), is satisfied when:

$$\max \delta(w^2) = 0 \tag{8}$$

The maximum of δ is attained when the wave number is a function of the prey diffusion. After deriving $\delta(w^2)$ and solving the derivative for w, we obtain the following value for the wave number.

$$w = \left(\frac{a_{22} - a_{11}}{D_y - D_x} + \frac{\left(-D_y D_x \left(D_y^2 - D_x^2 \right)^2 a_{12} a_{21} \right)^{\frac{1}{2}}}{D_y D_x \left(D_y - D_x \right)^2} \right)^{\frac{1}{2}} \tag{9}$$

or as w, as in Eq.(9). The wave numbers, Eq.(9) and Eq.(9), are important when studying the bifurcating uniform and periodic solutions, the type of eigenvalues encountered in one dimension is presented in Fig.(4) The shape of the eigenvalue in $2-Dim$ is presented in Fig 5. All the corresponding pattern formations across the two-dimensional system are given in Fig.(7) and they are also described in the discussion section.

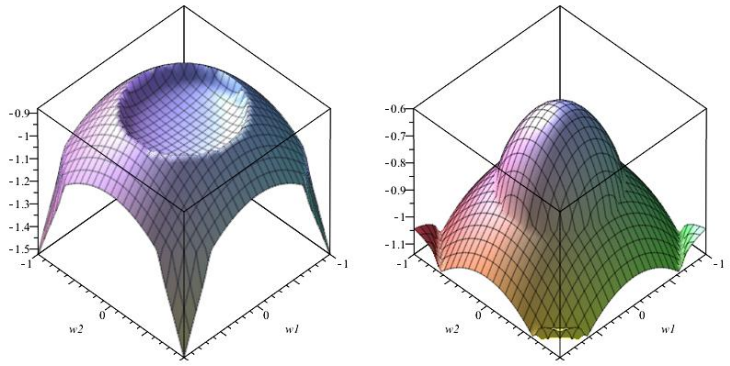

(a) (b)

Figure 5: The types of the eigenvalues present across two dimensions when $\theta = 3.5$ and $K = 120$ and all other parameter values are as in table 1. The results shown in these two figures are consistent with Fig.(4) when the diffusion parameter values are $D_x < D_y$ and the wave numbers between $-1 < w < 1$.

5.2. Analysis of one dimension

In this section, we studied Turing mechanism to specify at what point and under what conditions we obtain Turing patterns, we considered the same model and performed some numerical simulation to understand the behaviour of the reaction diffusion model as presented in 5.1.

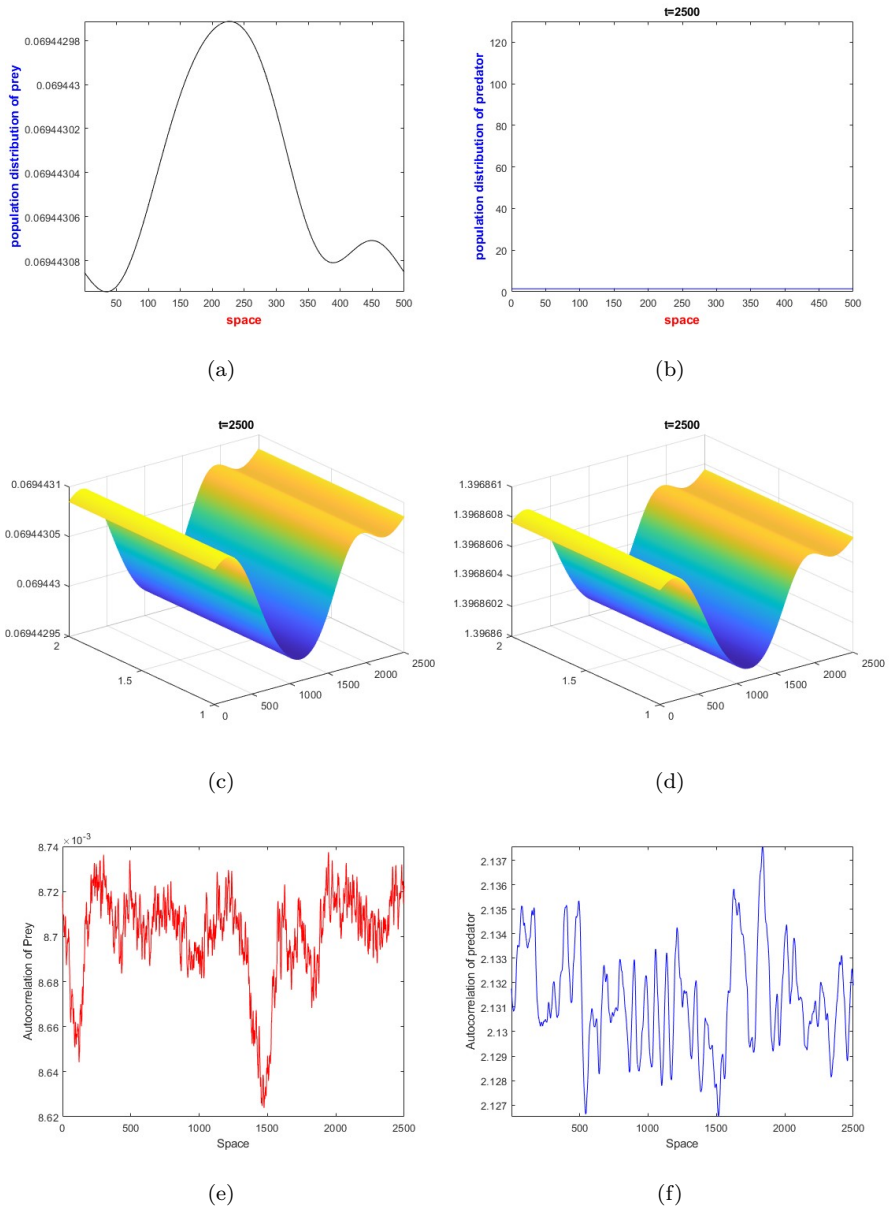

Figure 6: State of development for Turing patterns area in one dimension captured for different time series, the solution when $K = 120$, and $\theta = 3.5$ and $\delta = 0.75$ with stable focus equilibrium point, by choosing D_x less than $D_y = 0.5$ will change the stable steady state to unstable.

Next, is to clarify where is Turing bifurcation and Turing-Hopf bifurcation and the linearized system at (x_e, y_e) :

Theorem 5.1. *Assume delta* > 0.7*, there is Turing bifurcation for the diffusive model given in Eq.(1) with the critical Turing bifurcation curve* $\mu = \mu\left(\delta, w_*^2\right)$*, and Turing-Hopf bifurcation at the interaction point* (δ_H, μ_*) *with* $\mu_* = \mu\left(\delta_H, k_*^2\right)$*, where* $\mu\left(\delta_H, w_*^2\right)$ *is determined by Eq.(8) and* w_* *is determined by Eq.(9).*

Proof. For (x_1, y_1), we can easily obtain from $J_w = 0$, that spatial patterns can arise in correspondence of those modes w for which $Re(\lambda) > 0$ Since (x_1, y_1) is stable for the reaction system, one has that $tr(w) < 0$ and $tr(w^2) > 0$. Thus to obtain $Re(\lambda) > 0$ for some $w \neq 0$ is when $\lambda(w^2) < 0$. The following two conditions need to be satisfied:

(a) Determine the critical value of the wave number i.e. $w = w_c$, which is given in Eq.(8), by deriving $\delta(w^2)$.

(b) Determine the critical values of θ and w using Eq. (8), it is important to mention that the range of the spectrum is given by $w_1 < \delta < w_2$ depends on the third condition of pattern formation as in Eq. (10).

$$a_{11}D_y + a_{22}D_x - 2((D_xD_y)^{1/2})(a_{11}a_{22} - a_{12}a_{21})^{1/2} > 0, \tag{10}$$

The condition in Eq.(10) represent the onset of diffusion-driven instability and satisfying this condition can prove the system in Eq.(1) will exhibit Turing Hopf patterns.

i.e. $T_0 = 0, J_0 > 0$; and the transversality condition: $\left.\frac{dRe(\lambda)}{d\delta}\right|_{\delta=\delta_H} \neq 0.$

From $T_0 = a_{11} + a_{22}$, we obtain $\delta = \delta_H$, where:

$\delta_H = \frac{a_{11}\theta^2 + a_{22}\theta - a_{12}}{(ad-em)\theta - cd)^2 kcd}$.

$a_{11} = \frac{r}{\theta+x} - \delta x + \frac{x}{k} + x(-\frac{r}{(\theta+x)^2} - \delta + k^{-1}) - \frac{my}{ax+c} + \frac{mxya}{(ax+c)^2}$

$a_{12} = -\frac{mx}{ax+c}$.

$a_{21} = \frac{emy}{ax+c} - \frac{emxya}{(ax+c)^2}$

$a_{22} = \frac{emx}{ax+c} - d,$

When $\delta > \delta_H$, $T_0 < 0$, the corresponding ordinary differential system is asymp-

totically stable; when $\delta < \delta_H, T_0 > 0$ (here, $\theta > 3.5$ is required), the corresponding ordinary differential system is stable. Therefore, when $\delta = \delta_H, T_0 = 0$, the system occurs Hopf bifurcation near (x_1, y_1). Moreover, by virtue of $\mathrm{Re}(\lambda) = \dfrac{T_0}{2}$ and we judge that the system goes through the transition from stable to unstable.

6. Turing Instability

6.1. One Dimensional Spatial Distribution

In this section, we aim to discuss the possible patterns which may arise in the operation of a two-component spatial version of the predator–prey model, as presented in Eq.(1). Let's introduce the necessary diffusion parameters. The diffusion coefficients are denoted by D_x and D_y. These allow the inclusion of spatial diffusion terms corresponding to the horizontal plane, recalling Eq.(1). We impose for $X \in \Omega$, where Ω is a bounded region $[0, L]$, the condition that $t \in [0, \infty)$, $F(x, y)$ and $G(x, y)$ are all the same, as in Eq.(2) and Eq.(3). We assume $n\nabla^2(x, y)^T = 0$ on $\partial\Omega$, where $\partial\Omega$ is the closed boundary of the reaction diffusion domain, Ω, and n is the outward unit normal vector to Ω. Turing instability (diffusion-induced instability) means that in the absence of diffusion, the steady state solutions are stable, which becomes unstable with taking diffusion into account. In ODE systems, for the boundary steady state (x_0, y_0), we have zero flux boundary conditions; this implies a closed system—no species enter or leave the environment defined for this model. In this section, we carry out a mathematical analysis to observe the quantitative dynamics of the model presented in Eq.(1) but without making it dimensionless. For simplicity, and without loss of generality, we fix $D_y = 1$ and undertake a relative exploration concerning how the spatial dynamics change for a range of $D_x < D_y$. To solve the model in Eq.(3) numerically, we set the initial conditions as:

$$\begin{aligned} x(X, 0) &= x_e + \epsilon \cos(wX) \\ y(X, 0) &= y_e + \epsilon \sin(wX) \end{aligned} \tag{11}$$

for $X \in [0, L]$. Note also, however, that there are infinitely many solutions (i.e., eigenfunctions) to the spatial problem. The solution of the mathematical model will always depend on the initial conditions and parameters: small changes in the initial states (or parameters) of the system produce small changes in the outcome Hancock [2004]. The initial condition given by Eq.(11) is the approximate solution of Eq.(3). It has the term x_e,y_e as the exact solution of the system (a steady state) and the term $\epsilon \cos(wX)$ as the perturbation. w is the spectrum of (x_e, y_e), with Neumann boundary conditions as periodic boundary conditions: $\nabla x = 0$, $\nabla y = 0$ w.r.t x. The latter is a periodic function, and the above are considered to be the periodic boundary conditions that impose the weakest influence on pattern formation: i.e., a natural choice is to assume that the boundaries do not influence the interior of the domain and impose zero flux Gambino [2012] and Crampin [1999]. The first step in analyzing the model is to determine the equilibria (stationary states) of the non-spatial model obtained by setting the space derivatives to zero, and this has already been done and studied in detail in section 3; the results are presented for this context in the next section.

6.2. Turing patterns analysis

In this section we investigate the possibility of pattern emergence in the operation of Eq.(3). Through a linear stability analysis, we show that the co-existence point is stable for the reaction system but will become unstable for the reaction diffusion system. In the current work, we will always consider the stability of the equilibrium point defined by $x(t) = x_e$ and $y(t) = y_e$ in relation to Eq.(3) as corresponding to $dx/dt = dy/dt = 0$, the coexistence equilibria presented in Eq.(6). The other equilibria are linearly unstable so we exclude them from the current analysis. For the point (x_0, y_0) to be the coexistence steady state, linear conditions must be imposed. The linearized system in the neighborhood of (x_0, y_0) is:

$$\frac{\partial}{\partial t}\begin{pmatrix} x \\ y \end{pmatrix} = \begin{pmatrix} D_x & 0 \\ 0 & D_y \end{pmatrix} \nabla^2 \begin{pmatrix} x \\ y \end{pmatrix} + \begin{pmatrix} F(x,y) \\ G(x,y) \end{pmatrix} \tag{12}$$

Let U be a vector of (x, y) and u_e be a constant vector of (x_e, y_e), S.t $F(u_e) = 0$. Thus, we can define $\overline{U} = U - u_e$, and such a definition will lead to the following system:

$$\frac{\partial \overline{U}}{\partial t} = D\nabla^2 \overline{U} + F(u_e) + J\overline{U} \tag{13}$$

where $F(u_e) = 0$ and J is a Jacobian matrix.

$$\overline{U}_t = D\nabla^2 \overline{U} + J\overline{U}, \tag{14}$$

where we define,

$$\overline{U} = \begin{pmatrix} x \\ y \end{pmatrix} \tag{15}$$

$$D = \begin{pmatrix} D_x & 0 \\ 0 & D_y \end{pmatrix} \tag{16}$$

$$J\overline{U} = \overbrace{\begin{pmatrix} a_{11} - D_x w^2 & a_{12} \\ a_{21} & a_{22} - D_y w^2 \end{pmatrix}}^{J(w)} \tag{17}$$

where all Jacobian elements are given in section 5.2: The first stage of pattern formation can usually be investigated by finding a solution of Eq.(14). We can start with a linear stability analysis, linearising about a fixed point, (x_e, y_e);

Theorem 6.1. In the reaction diffusion model presented in Eq.(1), the spatiotemporal values are defined under Neumann boundary conditions:

$$X = \left\{ x \in \left(y^{2,2}(0, l\pi) \right)^2, \frac{\partial x_i}{\partial \tau} = 0, \pi, i = 1, 2 \right\}$$

Using inner product

$$[x, y] = \int_0^{l\pi} (x_1 y_1 + x_2 y_2)\, dx, x = (x_1, x_2)^T, y = (y_1, y_2)^T \in X$$

in this theorem, we introduce two perturbation parameter $\varepsilon = (\varepsilon_1, \varepsilon_2) \in \mathbb{R}^2$, due to the fact that Turing-Hopf bifurcation is a co-dimension-2 bifurcation, where $\varepsilon_1 = \theta - \theta_*, \varepsilon_2 = \delta - \delta_*$. Let $\theta_* = \theta_H$, I define the bifurcation point of

the system is $\varepsilon = 0$. Let's rewrite (x_1, y_1) in the form of bifurcation parameters, denoted by $(x_e(\varepsilon_1), y_e(\varepsilon_1))$ as follows:

$$\begin{aligned} x &= x_e + \epsilon e^{\sigma t + i(w_1 x + w_2 y)} \widetilde{x}, \\ y &= y_e + \epsilon e^{\sigma t + i(w_1 x + w_2 y)} \widetilde{y}, \end{aligned} \tag{18}$$

after following the same procedures in the earlier section, we will determine the following dispersion (characteristic equation):

$$\begin{aligned} \sigma^2 - \delta \left(D_x + D_y\right] w_1^2 - \left[D_x + D_y w_2^2 - a_{11} - a_{22}\right) \\ + D_x D_y (w_1^4 + w_2^4) + 2 D_y D_x a_{11} (w_1^2 w_2^2) + D_x a_{22} (w_1^2 + w_2^2) \\ + D_y a_{11} (w_1^2 + w_2^2) + Det(J) = 0. \end{aligned} \tag{19}$$

Solving Eq. (19) will give the spectrum of the model in two dimensions, which helps us to figure out the system stability and show the consistency between the two dimensional spatial model analysis. where,

$$H(w^2) = ([a_{11} - D_x w^2][a_{22} - D_y w^2]) - a_{12} a_{21} \tag{20}$$

proof: the coexistence point (x_e, y_e) is stable in relation to the spatially homogeneous mode $w = 0$ entails that $tr(J) < 0$ and $det(J) > 0$. In order to have diffusion driven instability, we require $Re(\sigma) > 0$ for some $w \neq 0$, and this is equivalent to imposing $H(w^2) < 0$ for some $w \neq 0$. Since $H(w^2)$ is symmetric around the origin, the above condition holds and requires that $D_P a_{11} + D_M a_{22} > 0$. Finally, for diffusion-driven instability to occur, we also require that there exist real w^2 such that $H(w^2) = 0$. It is easily shown that this yields to the imposition of $(D_x a_{11} + D_y a_{22})^2 - 4 D_x detJ > 0$, whereby diffusion driven instability arises and spatial patterns can develop; this is given for a particular choice of the other system parameters Murray [2003]. In relation to dispersion relations of the form $\sigma = \sigma(w)$ stemming from Eq.(20), the sign of the real part of σ indicates whether the solution will grow or decay over time. If the real part of $\sigma(w)$ is negative for all w values, then any superposition of

solutions of the form $\exp^{(\sigma t+iwx)}$ will also appear to decay. On the other hand, if the real part of $\sigma(w)$ is positive for some values of w, then over time some components of a superposition will grow exponentially. The former case is called stable, whereas the latter is termed unstable. If the maximum of the real part of δ is exactly zero, the situation is called marginally stable. It is more difficult to assess the long term behaviour in the above case. The basic linear algebra can lead us to derive the stability conditions using the parameter values given in Table 1. To obtain some conditions we must connect the main parameter θ with the other system parameters Murray [2003]. From the Turing first condition, $a_{11} + a_{22} < 0$ where a_{11} and a_{22} are elements of the Jacobian matrix given in section 5.2, to obtain the condition for θ, it is worth noting that trace(J) is a quadratic equation in θ and both roots are positive. Thus, we obtain that $\theta > 0$ when the prey diffusion parameters $0 < D_x < 0.5$ and $D_y = 1$ so the mobility condition is satisfied $\frac{D_x}{D_y} < 1$.

7. Results

The model defined by Eq.(3) is based on an original idea investigated in Rosenzweig–MacArthur predator–prey model Rosenzweig [1963] and first discussed in Zu [2010]. When there is a shortage of mates so that the regeneration rate of the prey species is limited, this won't impact the mortality compensation ratio and will introduce an Allee effect on prey growth kuussaari [1998]. We undertook a quantitative analysis of the non-local interactions of the above system, using the Turing mechanism. We studied the dynamical behaviour of the general spatio–temporal predator–prey system: at least, that which could be reduced in order to fit in the model studied Lewis *et al.* [2012] (when setting $\theta = 0$). In the operation of Eq.(1), we observed robust processes in the represented marine ecosystem which we believe are critical to the understanding of prey bloom formation. We observed, see Sec. 5.1, that when the rate of interaction, i.e., U_e, crosses a threshold value, both species populations start oscillating

around a single interior equilibrium. This is due to Hopf-Turing pattern, which may appear for both parameter cases (θ, δ) due to complex eigenvalue in uniform solution (Hopf bifurcation) and instability region for the periodic state when we introduce a diffusion term. We summarize the uniform and periodic solution (in time and space) behaviour shown numerically in Sec. 6.1 for different values of U_e. We also simulate several bifurcation diagrams for several parameter θ for both cases. The results show that the periodic states only exist in $0 \leq \theta \leq 3.5$ regime. Spatial patterns can arise in correspondence with those modes, w, for which $Re(\delta) > 0$. Since (U_e) is stable for the reaction system, then $tr(w) < 0$ and $det(J) > 0$, as shown in Fig 4 and 5, across one and two dimensions respectively. The solution of the system becomes unstable when the prey diffusivity is set to $D_p = 0.5$; this will lead to unstable behaviour. For example, in Fig 6, the solution of the system becomes unstable when the prey diffusivity is set to $D_p = 0.5$ or even less; this leads to the emergence of an unstable area under the stability curve. When choosing another value for θ and in order to reach another, corresponding, equilibrium point, e.g., when choosing $\theta = 3.5$ and its corresponding equilibrium point, we find that this is also stable, but only when $D_p = 0.5$, which means that the area above the stability curve is stable. We found that because of the local interaction in the temporal system and its corresponding roots, the region can exhibit another stability. Fig 7 shows the different patterns related to $\theta = 3.5$ which were trialled. In Figs 7(a), 7(c), 7(d), 7(b), we have Turing-Hopf patterns when $D_x = 0.5$, $\theta = 3.5$ and $k = 120$, with all other parameter values as in Table 1. Turing patterns are presented in Fig8 with the same parameter values as in Table 1, $\theta = 3.5$, $\delta = 0.75$ and $k = 120$. Our numerical approach has helped us to discover the outcomes of the Allee effect, which is probably an unstable factor in the food web; in fact, θ and δ acts as a control parameters with respect to the system's qualitative behaviour and so facilitates an investigation into the stability and the dynamics of the system via the phase plane tool presented in Figs. (3). For instance, by setting $\theta = 0$, we reduce the system so that it is more likely to be similar to the Rosenzweig-MacArthur model, Kot [2001], and this means that the sys-

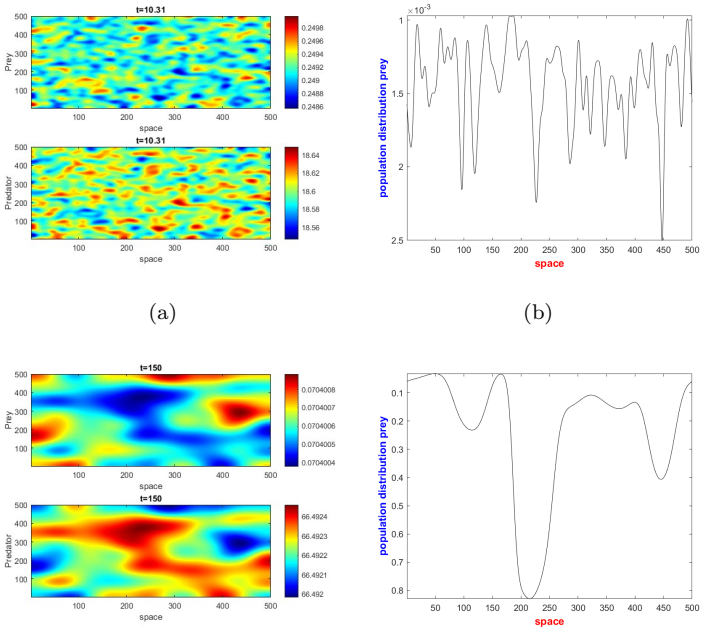

(a) (b)

(c) (d)

Figure 7: The behaviour of the system across two dimensions when $\theta = 3.58$, $\delta = 0.75$ and $k = 120$ and the parameter values are set as in table 1. Both Fig.(7(a)) and Fig.(7(c)) reflect the fluctuations of Turing Hopf in the prey and predator populations when $\theta < 1$, i.e., relatively small.

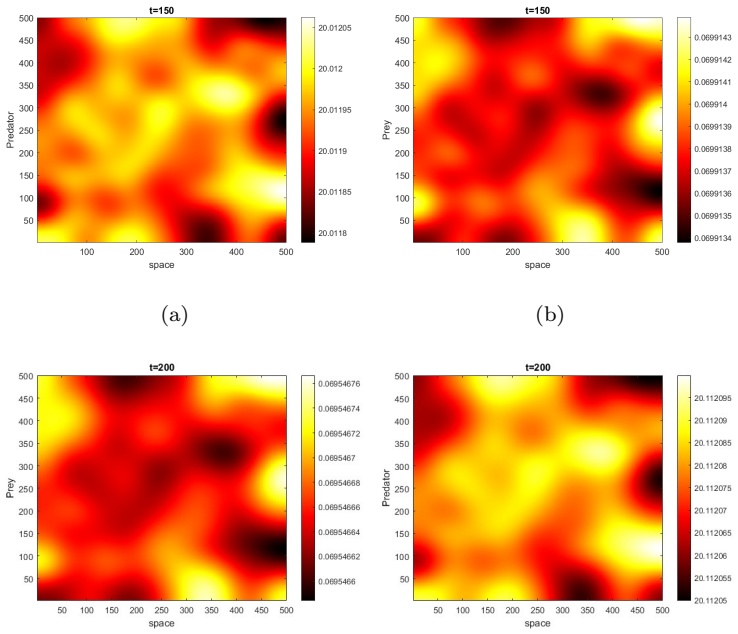

(a) (b)

(c) (d)

Figure 8: The behaviour of the system across two dimensions when $\theta = 3.58$, $\delta = 0.25$ and $k = 1000$ and the parameter values are set as in table 1. Both Fig.(8(a)) and Fig.(8(b)) reflect Turing patterns in the the prey and predator populations when $\theta < 1$, i.e., relatively small.

tem will be unstable and will show periodic cycles in terms of the densities of predator and prey. Abrams *et al.* [1996] and Truscott *et al.* [1994] considered interactions between prey and predator which create a situation whereby the system possesses a stable equilibrium whose solution trajectories perform large oscillations before returning to that equilibrium. Increasing and decreasing the value representing the Allee effect (the control parameter, θ) will result in there being various differing cases in terms of stability and various different patterns, as shown in the stability (bifurcation) diagram Fig.(3). In association with this, we obtained a variety of different Turing patterns shown in Fig.(7), which corresponded to $\theta = 3.5$ This explains how Allee effect provides a mechanism for increasing predation on prey. The detailed analysis in this article is consistent with the numerical findings in Zu [2010] in relation to the situation where $k = 120$, $0 < \theta < 3.5$ and $0 < \delta < 0.75$.

8. Conclusion and Discussion

All the results presented in section 7 demonstrate the operation of the predator–prey model mentioned in Zu [2010]. The main aim of this article, however, is to develop analytical expressions and numerical representations for the model presented in spatial terms via Eq.(1) and in temporal terms via Eq.(3). This presentation is focused on the curve that describes the bifurcation behaviours, and then is further illustrated using a specific set of parameters. The set of parameters given in table 1 allows a wide range of behaviours to be observed with respect to a relatively small θ parameter space. The types of stability of the system fall into three categories, based on the predator–prey population, as given in table 2. Two 'unstable node' oscillates away from the initial condition, yielding population oscillations that grow without bound. A 'stable centre' indicates a closed loop, where population oscillations stay steady without damping until both populations remain steady. There is an extra instability (not at the coexistent point). The 'phase plane' technique is a standard method used to produce graphical representations of the dynamics of two component systems (a

phase portrait). The technique is described in detail by Kot [2001] and Britton [1986]. In terms of local interactions, we investigate the impact of the Allee effect on the stability of a predator–prey system when prey population is subject to such an effect. We show that a predator–prey model taking account of the Allee effect may admit Turing Hopf bifurcations, as shown in Fig.(3). In Fig. (2), it can be seen from the time independent analysis that there were periodicity in both the predator and the prey populations, see Fig.(2(a)). Fig.(2(e)) links the reason for this to the equilibrium type (being 'stable focus'); this represents the instability that can take place even when an infinitely large carrying capacity, $k = 120$, is assumed in the model. Investigations were carried out to look at the small fluctuations in both species' populations evident from the one-dimensional analysis as shown in Fig.(6). These fluctuations cause nonuniform prey, activator species densities. This elevated prey density has a positive effect both on prey and predator population growth rates Alonso *et al.* [2002]. Looking at the per capita rates in Eq.(3), it can be seen that some cases of sudden extinction of species have occurred –in situations where there were 'safe' numbers initially. Finally, using our spatiotemporal model, we have addressed the issue of Turing Patterns. Spatiotemporal chaotic patterns exist with respect to the parameter values given in Table 1. These observations confirm the idea that the interaction between the temporal and spatial instabilities are unable to drive the system towards spatial and temporal irregularity under any circumstances. In relative terms, the existence of irregular distributions of populations over space and the continuous changes with time of these depend on the complex interactions is taking place over spatial and temporal scales. The current study is in agreement with previous studies which were carried out to try to explain the reason behind such fluctuation phenomena; it has been established mathematically that these are caused by changes from steady state equilibria to unsteady state equilibria due to Hopf bifurcation bifurcation Boettiger [2012], Scheffer [2009]. Another reason, as established by schreiber [2003], is the existence of long-living species.

9. Appendix

- The cascading parameters of Eq.7 are given as follows:

$$A = 4ka^6d^6em - 24ka^5d^5e^2m^2 + 60ka^4d^4e^3m^3 - 80ka^3d^3e^4m^4 + 60ka^2d^2e^5m^5 - 24kade^6m^6 + 4ke^7m^7 + a^6cd^6 - 2a^5cd^5em - a^4cd^4e^2m^2 + 4a^3cd^3e^3m^3 - a^2cd^2e^4m^4 - 2acde^5m^5 + ce^6m^6. \quad (21)$$

$$B = 4D_x^2k^2a^4w_1^4x^5 + 4D_x^2k^2a^4w_2^4x^5 + 16D_xka^4w_1^2x^6 + 16D_xka^4w_2^2x^6 + 4D_x^2k^2c^4w_1^4x + 4D_x^2k^2c^4w_2^4x + 4k^2a^4d^2x^5 + 4k^2a^4drx^5 + 4k^2a^2e^2m^2x^5 + 16k^2a^3cd^2x^4 - 16ka^4dx^6 - 8ka^4rx^6 + 16ka^3emx^6 + 4k^2a^4x^5 + 24k^2a^2c^2d^2x^3 - 16ka^4x^6 + 16a^4x^7 + 4k^2c^4d^2x - 96ka^2c^2x^4 + 8k^2c^4dx + 4k^2c^4rx - 64kac^3x^3 - 16kc^4dx^2 - 8kc^4rx^2 + 4k^2c^4x - 16kc^4x^2 + 16c^4x^3. \quad (22)$$

$$C = D_x^2k^2a^4w_1^4x^4 + D_x^2k^2a^4w_2^4x^4 + 2k^2a^4dx^8 + 2k^2a^4rx^8 + 4D_xka^4w_1^2x^5 + 4D_xkx^5 + 4k^2a^3cx^7 - 16ka^3cx^8 + D_x^2k^2c^4w_1^4 + 2D_x^2k^2c^4w_1^2w_2^2 + D_x^2k^2c^4w_2^4 + k^2a^4d^2x^4 + 6k^2a^2c^2x^6 + k^2a^2e^2m^2x^4 + 8k^2ac^3rx^5 - 2k^2c^3emx^5 - 24ka^2c^2x^7 + 4k^2ac^3x^5 + 2k^2c^4dx^4 - 16kac^3x^2 - 4kc^4dx - 4kc^4x + 4c^4x^2 + 96k. \quad (23)$$

$$D = 2k^2c^4rx^4 - 2k^2c^3mx^4y - 4ka^4dx^5 + 4ka^3emx^5 - 16kac^3x^6 - 2D_xk^2c^4dw_1^2 - 2D_xk^2c^4dw_2 + 6k^2a^2c^2d^2x^2 + k^2c^2e^2m^2x^2 - 4ka^4x^5 + 4a^4x^6 + k^2c^2m^2y^2 - 24ka^2c^2x^3 + 2k^2c^4d - 2k^2c^3 - 4ar^2dx - 4km^2x + 4k^2x + 56k. \quad (24)$$

$$E = k^2a^3cr^2x^7 + 4ka^3emx^9 + 6k^2a^2c^2d^2x^6 + 6k^2a^2c^2r^2x^6 + k^2c^2e^2m^2x^6 - 16ka^3cdx^8 - 16ka^3crx^8 + 4D_xkc^4w_1^2x^5 + 4D_xkc^4w_2^2x^5 + 4k^2ac^3d^2x^5 + 4k^2ac^3r^2x^5 - 24ka^2c^2dx^7 - 24ka^2c^2rx^7 + D_x^2k^2a^4w_1^4x^8 + D_x^2k^2a^4w_2^4x^8 + 4D_xka^4w_1^2x^9 + 4D_xka^4w_2^2x^9 + D_x^2k^2c^4w1^4x^4 + D_x^2k^2c^4w_2^4x^4. \quad (25)$$

- The coefficients of quartic polynomial polynomial in Eq.(7):

$$\alpha_1 Z^5 + \alpha_2 Z^4 + \alpha_3 Z^3 + \alpha_4 Z^2 + \alpha_5 Z + \alpha_6 = 0$$

$$\alpha_1 = 2D_y a^2 w_1^2 + 2a^2 d + 2a^2 - 2aem \tag{26}$$

$$\begin{aligned}\alpha_2 = {} & D_y D_x k a^2 w_1^4 + D_y k a^2 w_1^2 - D_y k a^2 r w_1^2 + D_x k a^2 d w_1^2 + D_x k a^2 w_1^2 \\ & - D_x k a e m w_1^2 + 4D_y a^2 \theta w_1^2 + 4D_y a c w_1^2 + k a^2 (d - dr + 1 - r) - k a e m (1 + r) \\ & + 4a^2 d\theta + 4a^2 \theta - 4aem\theta + 4acd + 4ac - 2cem \end{aligned} \tag{27}$$

$$\begin{aligned}\alpha_3 = {} & 2D_x k a^2 \theta w_1^4 + 2D_y D_x k a c w_1^4 + 2D_y k a^2 \theta w_1^2 - 2D_y k a^2 r \theta w_1^2 \\ & + 2D_x k a^2 d\theta w_1^2 + 2D_x k a^2 \theta w_1^2 - 2D_x k a e m \theta w_1^2 + 2D_y a^2 \theta^2 w_1^2 \\ & + 2D_x k a c d w_1^2 + 2D_x k a c w_1^2 - D_x k c e m w_1^2 + 8D_y a c \theta w_1^2 \\ & + 2k a^2 d\theta - 2k a^2 dr\theta + 2k a^2 \theta - 2k a^2 r\theta - 2k a e m \theta (1 + r) + 2D_y c^2 w_1^2 \\ & + 2kacd - 2kac(dr + c - r) + 4a^2 d\theta^2 - 2aem\theta^2 + 8acd + ac\theta - 4cem\theta + 2c^2 d + 2c^2. \end{aligned} \tag{28}$$

$$\begin{aligned}\alpha_4 = {} & D_y D_x k a^2 \theta^2 w_1^4 + 4D_y D_x k a c \theta w_1^4 + D_y D_x k c^2 w_1^4 + D_y k a^2 \theta^2 w_1^2 \\ & + D_x k a^2 d\theta^2 w_1^2 + D_x k a^2 \theta^2 w_1^2 - D_x k a e m \theta^2 w_1^2 + 4D_y k a c \theta w_1^2 - 4D_y k a c r \theta w_1 \\ & + 4D_x k a c d \theta w_1^2 + 4D_x k a c \theta w_1^2 - 2D_x k c e m \theta w_1^2 + D_y k c^2 w_1^2 - D_y k c^2 r w_1^2 + D_y k c m w_1^2 y \\ & + 4D_y a c \theta^2 w_1^2 + D_x k c^2 d w_1^2 + D_x k c^2 w_1^2 + k a^2 d\theta^2 + k a^{22} \theta^2 - k a e m \theta^2 \\ & + 4D_y c^2 \theta w_1^2 + 4kacd\theta - 4kacdr\theta + 4kac^2\theta - 4kacr\theta - 2kcem\theta(1 + r) + kc^2 d(1 - r) \\ & + kcy(D_y + m) + \theta c(4ad + 4a - 2em + 4d) - \theta + 4c^2. \end{aligned} \tag{29}$$

$$\begin{aligned}\alpha_5 = {} & 2D_y k a c \theta^2 w_1^4 + 2D_y k c^2 \theta w_1^4 + 2D_y k a c \theta^2 w_1^2 + 2k a c d \theta^2 w_1^2 \\ & + 2k a c \theta^2 w_1^2 - k c e m \theta^2 w_1^2 + 2D_y k c^2 \theta w_1^2 - 2D_y k c^2 r \theta w_1^2 + 2D_y k c m \theta w_1^2 y \\ & + 2kcd\theta w_1 + 2kc^2 \theta w_1^2 + 2D_y c^2 \theta^2 w_1^2 + 4kacd\theta^2 \\ & - kcem\theta^2 - 2kc^2 dr\theta + 2kc^2\theta - 2kc^2 r\theta + 2kcD_y \theta y \\ & + 2kcm\theta y + 2c^2 d\theta^2 + 2c^2\theta^2 \end{aligned} \tag{30}$$

$$\alpha_6 = \theta^2(D_x kc^2 w_1 + kc^2 w_1^2 + kcmw_1^2 y + D_x kc^2 dw_1^2 + D_x kc^2 w_1^2 + kc^2 d + kc^2 + kcm(d+1)) \tag{31}$$

References

Abrams, Peter A and Walters, Carl J (1996) Invulnerable prey and the paradox of enrichment. vol 77, 4:1125–1133, journal of Ecology, Wiley Online Library.

Kot M, (2001) Elements of mathematical ecology, Cambridge University Press.

Turing, A (1952) Philosophical the royal biological transqfctions society sciences, Phil. Trans. R. Soc. Lond. B, vol. 237, pages 37–72.

Alonso, David and Bartumeus, Frederic and Catalan, Jordi (2002) Mutual interference between predators can give rise to Turing spatial patterns, Ecology, volume 83, pages 28–34, Wiley Online Library.

Baurmann and Ebenhoh, M , W and Feudel, U (2004) Turing instabilities and pattern formation in a benthic nutrient-microoganism system, Mathematical biosciences and engineering: MBE, pages 111-130.

Banerjee, Sudipto and Carlin, Bradley P and Gelfand, Alan E (2014), Hierarchical modeling and analysis for spatial data, Crc Press.

Boettiger, Carl and Hastings, Alan (2012), Quantifying limits to detection of early warning for critical transitions, Journal of the Royal Society Interface, volume 9, pages 2527–2539, The Royal Society.

Britton, Nicholas Ferris (2003), Population dynamics of interacting species, Essential Mathematical Biology, pages 47–82, Springer.

Britton, Nicholas F and others (1986), Reaction-diffusion equations and their applications to biology, Academic Press.

Courchamp, F and Grenfell, B and Clutton-Brock, T (1999), Population dynamics of obligate cooperators, Proceedings of the Royal Society of London. Series B: Biological Sciences, pages 557–563, The Royal Society.

Crampin, Edmund J and Gaffney, Eamonn A and Maini, Philip K (1999), Reaction and diffusion on growing domains: scenarios for robust pattern formation, Bulletin of mathematical biology, volume 61, pages 1093–1120, Springer.

Edwards, Andrew M and Brindley, John (1996), Oscillatory behaviour in a three-component plankton population model Dynamics and stability of Systems, volume 11, pages 347–370.

Ferdy, Jean-Baptiste and Molofsky, Jane (2002), Allee effect, spatial structure and species coexistence, Journal of theoretical Biology, volume 217, pages 413–424, Elsevier.

Franks, Peter JS, (2002) NPZ models of plankton dynamics: their construction, coupling to physics, and application. Journal of Oceanography, 58:379–387, Springer.

Elragig, Aiman and Townley, Stuart (2012), A new necessary condition for Turing instabilities, Mathematical biosciences, volume 239, pages 131–138, Elsevier.

Neubert, Michael G and Caswell, Hal and Murray, JD (2002), Transient dynamics and pattern formation: reactivity is necessary for Turing instabilities, Mathematical biosciences, volume 175, pages 1–11, Elsevier.

Zhou, Shu-Rong and Liu, Ya-Feng and Wang, Gang (2005), The stability of predator–prey systems subject to the Allee effects, Theoretical Population Biology, volume 67, pages 23–31, Elsevier.

Zu, Jian and Mimura, Masayasu (2010), The impact of Allee effect on a predator–prey system with Holling type II functional response, Applied Mathematics and Computation, volume 217, pages 3542–3556, Elsevier.

Kent, Adam and Doncaster, C Patrick and Sluckin, Tim (2003), Consequences for predators of rescue and Allee effects on prey, Ecological Modelling, volume 162, pages 233–245, Elsevier.

Morozov, Andrew and Arashkevich, Elena and Nikishina, Anastasia and Solovyev, Konstantin, (2010) Nutrient-rich plankton communities stabilized via predator-prey interactions: revisiting the role of vertical heterogeneity,

Mathematical medicine and biology: Journal of the IMA, 28:185–215, Oxford University Press.

Kuussaari, Mikko and Saccheri, Ilik and Camara, Mark and Hanski, Ilkka (1998), Allee effect and population dynamics in the Glanville fritillary butterfly, Oikos, pages 384–392, JSTOR.

Edwards, Andrew M and Yool, Andrew, (2000) The role of higher predation in plankton population models. Journal of Plankton Research, volume 22, pages 1085–1112, Oxford Univ Press.

Edwards, Christopher A and Batchelder, Harold P and Powell, Thomas M (2000), Modeling microzooplankton and macrozooplankton dynamics within a coastal upwelling system. Journal of Plankton Research, volume 22, pages 1619–1648, Oxford Univ Press.

Edwards and Brindley, John, Andrew M, (1999) Zooplankton mortality and the dynamical behaviour of plankton population models. Bulletin of mathematical biology, 61:303–339, Springer.

Gambino and Lombardo, MC and Sammartino, M (2013), Pattern formation driven by cross-diffusion in a 2D domain. Nonlinear Analysis: Real World Applications, volume 14, pages 1755–1779, Elsevier.

Gambino and Lombardo, G, MC and Sammartino, M (2012), Turing instability and traveling fronts for a nonlinear reaction–diffusion system with cross-diffusion. Mathematics and Computers in Simulation, volume 82, pages 1112–1132, Elsevier.

Groom, Martha J (1998), Allee effects limit population viability of an annual plant, The American Naturalist, volume 151, pages 487–496. The University of Chicago Press.

Hansen B. and Tande, KS and Berggreen, UC, (1990) On the trophic fate of Phaeocystis pouchetii (Harlot). III. Functional responses in grazing demonstrated on juvenile stages of Calanus finmarchicus (Copepoda) fed diatoms

and Phaeocystis. Journal of Plankton Research, 12:1173–1187, Oxford Univ Press.

Haque, Mainul (2011) A detailed study of the Beddington–DeAngelis predator–prey model, vol.234, 1:1–16 Mathematical Biosciences, Elsevier.

Hancock, Matthew J (2004), The 1-D Heat Equation.

Rubao and Stegert, Ji, Christoph and Davis, Cabell S (2012), Sensitivity of copepod populations to bottom-up and top-down forcing: a modeling study in the Gulf of Maine region. Journal of Plankton Research, volume 35, pages 66–79, Oxford University Press.

Lewis ND, Breckels MN and Steinke M and Codling EA, (2013) Role of infochemical mediated zooplankton grazing in a phytoplankton competition model, Ecological complexity, vol 16:41–50, Elsevier. passengers?. Zoo biology, 5(2), pp.101-113.

Liermann, Martin and Hilborn, Ray (2001), Depensation: evidence, models and implications. Fish and Fisheries , volume 2, pages 33-58.

Lewis ND, Breckels MN, Archer SD, Morozov A, Pitchford JW, Steinke M, Codling, EA, (2012) Grazing-induced production of DMS can stabilize food-web dynamics and promote the formation of phytoplankton blooms in a multitrophic plankton model. Biogeochemistry 110, 303–313.

Muniyagounder and Balachandran, Sambath, Krishnan and Suvinthra, Murugan (2016), Stability and Hopf bifurcation of a diffusive predator-prey model with hyperbolic mortality. Complexity, volume 21, pages 34–43, Wiley Online Library.

Murray, J D (2003), Mathematical Biology II: Spatial Models and Biomedical Applications. Springer, New York, NY, USA.

Rodrigues, Luiz Alberto Díaz and Mistro, Diomar Cristina and Petrovskii, Sergei (2011), Pattern formation, long-term transients, and the Turing–Hopf

bifurcation in a space-and time-discrete predator–prey system. Bulletin of mathematical biology, volume 73, pages 1812–1840, springer.

Rosenzweig, Michael L and MacArthur, Robert H (1963), Graphical representation and stability conditions of predator-prey interactions, The American Naturalist, volume 97, pages 209–223, Science Press.

Rosenzweig, Michael L and others (1971), Paradox of enrichment: destabilization of exploitation ecosystems in ecological time, Science, volume 171, pages 385–387.

Saiz, Enric and Calbet, Albert, (2007) Scaling of feeding in marine calanoid copepods. Limnology and Oceanography, 52:668–675, Wiley Online Library.

Scheffer, Marten and Bascompte, Jordi and Brock, William A and Brovkin, Victor and Carpenter, Stephen R and Dakos, Vasilis and Held, Hermann and Van Nes, Egbert H and Rietkerk, Max and Sugihara, George (2009), Early-warning signals for critical transitions, volume 461, pages 53–59, Nature Publishing Group.

Schreiber, Sebastian J (2003), Allee effects, extinctions, and chaotic transients in simple population models. Theoretical population biology, volume 64, pages 201–209, Elsevier.

Truscott and Brindley, J, JE (1994) Ocean plankton populations as excitable media. vol 56, 5:981–998,Bulletin of Mathematical Biology, Elsevier.

Turing, Alan Mathison (1990), The chemical basis of morphogenesis. Bulletin of mathematical biology, volume 52, pages 153–197. Elsevier.

Wiggins, Stephen and Wiggins, Stephen and Golubitsky, Martin (1990), Introduction to applied nonlinear dynamical systems and chaos. Springer.

Ji, Chunyan and Jiang, Daqing and Shi, Ningzhong (2009), Analysis of a predator–prey model with modified Leslie–Gower and Holling-type II schemes with stochastic perturbation. Journal of Mathematical Analysis and Applications, volume 359, pages 482–498. Elsevier.